PAPER • **OPEN ACCESS**

Numerical prediction of efficiency and cavitation for a Pelton turbine

To cite this article: D Jošt *et al* 2019 *IOP Conf. Ser.: Earth Environ. Sci.* **240** 062033

View the article online for updates and enhancements.

IOP ebooks™

Bringing you innovative digital publishing with leading voices to create your essential collection of books in STEM research.

Start exploring the collection - download the first chapter of every title for free.

This content was downloaded from IP address 151.49.160.23 on 30/03/2019 at 10:32

IOP Conf. Series: Earth and Environmental Science **240** (2019) 062033 doi:10.1088/1755-1315/240/6/062033

Numerical prediction of efficiency and cavitation for a Pelton turbine

D Jošt[1], A Škerlavaj[1], V Pirnat[1], M Morgut [2], E Nobile[2]

[1] Kolektor Turboinštitut, Rovšnikova 7, 1210 Ljubljana, Slovenia

[2] University of Trieste, Department of Engineering and Architecture, Italy

E-mail: dragica.jost@kolektor.com

Abstract The first part of the paper illustrates the set-up and the methodologies adopted for the numerical analysis of the flow in a 6-jet Pelton turbine with vertical axis. At first, steady state simulations of flow in a distributor for three positions of needle stroke were performed. The results were used for the calculation of flow energy losses, analysis of jet quality and setting inlet boundary conditions for runner analysis. Runner analysis was done only for the maximal opening. The purpose of runner analysis for the model size was efficiency prediction. Numerical results were validated with the results from the test rig. Simulations for the prototype were done in order to check whether water sheets evacuating from the buckets impact the previous bucket and whether there is any interaction between the evacuating water sheets and the incoming jets. Analysis was done also for one nozzle operation. In the second part of the paper cavitation prediction for the prototype of a 2-jet Pelton turbine is presented. The problem, because of computational cost, was reduced to five runner buckets and one jet. A multiphase flow consists of water, air and water vapour. For cavitation pitting the vapour has to stick to the buckets and mass transfer from vapour to water has to happen in a very short time without the presence of air. With detailed analysis of numerical results it was concluded that in this case no cavitation pitting is expected.

1. Introduction

Compared to Kaplan and Francis turbines, complete CFD analysis of Pelton turbines is, because of the complex two phase flow, far more difficult and more time consuming. For this reason the first useful results were obtained relatively late. In 2002 Parkinson et al. [1] described a water jet from a Pelton turbine injector on the basis of experimental and numerical results. One of the first attempts to calculate free surface flow in a rotating bucket was done by Kvinsky et al. [2]. A bucket flow simulation using three adjacent buckets with efficiency prediction was illustrated by Mack and Moser [3]. Perrig [4] investigated flow in buckets by unsteady onboard wall pressure measurements, high-speed onboard and external flow visualizations, water film thickness measurements and CFD simulations. Efficiency prediction for a 2-jet Pelton turbine at different operating regimes was presented by Jošt at al. [5]. The effect of grid refinement and the importance of accurate description of real jet prescribed at the runner inlet, instead of the theoretical one, was emphasized. A great step forward was done by Santolin et al. [6]. They performed the simulation of an entire single-jet Pelton turbine. The runner was coupled with the final part of the penstock and the needle nozzle. The negative effect of the real jet, perturbed by the needle wake and secondary flows, in comparison with an ideal theoretical jet, was presented. In an attempt to overcome the mesh difficulties of the VOF

Content from this work may be used under the terms of the Creative Commons Attribution 3.0 licence. Any further distribution of this work must maintain attribution to the author(s) and the title of the work, journal citation and DOI.
Published under licence by IOP Publishing Ltd

method, the analysis by Marongiu et al. [7] was performed with a particle-based method. Its main drawback was a significant increase of computational time. A new approach was presented by Vessaz et al. [8]. They validated Finite Volume Particle Method (FVPM) and showed that it was an accurate tool to capture the deviation of high-speed water jets by rotating Pelton buckets. With increasing number of particles the accuracy of results was improved, so the method proved to be stable and consistent. The disadvantage of the method is, again, a long computing time. In addition, the discrepancy between calculated and measured values of torque was significant. Regarding the cavitation prediction an important achievement was reported by Rossetti at al. [9]. They presented a simulation of cavitating flow in a Pelton runner and suggested a practical criterion for risk assessment of cavitation pitting.

In this paper a numerical analysis for a 6-jet Pelton turbine that operates at 400 m head is presented. Contrary to the paper [5], where most of the effort was dedicated to the efficiency prediction at different operating regimes, in this paper the efficiency was calculated only at one operating point, for both the model and the prototype. The main purpose of this part of the study was to check the quality of the jets and in particular to see whether there is any interaction between the evacuating water sheets and the jets.

In the second part of the paper a numerical simulation of cavitating flow in the runner of a high head 2-jet Pelton turbine is presented. Careful inspection of results has been done in order to check whether the conditions for cavitation pitting are fulfilled and subsequent erosion can be expected.

2. Numerical set-up and computational meshes

The numerical analysis was performed with ANSYS CFX, Release 15.5 and Release 18.2. Turbulence was modelled with the k-ω SST model, and in one case also with the SAS SST model. The advection term was discretized with the high resolution scheme (HRS) implemented in ANSYS CFX code. For time discretization the second order Euler scheme was used.

Multiphase flow was modelled with the homogeneous model. For mass transfer from water to vapour and vice versa the standard Zwart mass transfer model [10] was used.

Due to complex geometry a combination of structured and unstructured meshes was used. Basic mesh for manifold with injectors and jets consisted of 14.2 million elements with 12.6 million nodes. After the refinement in the injectors and in the regions with jets the mesh consisted of 31.9 million elements with 20.4 million nodes (see figure 1). For runner analysis the computational domain was reduced to one half due to the symmetry. The unstructured grid consisted of about 46 million elements with 21 million nodes. A detail of the grid can be seen in figure 2.

For cavitation prediction the problem was reduced to five runner buckets and one jet. Unstructured mesh was rather coarse in the regions without buckets and significantly refined on the buckets, especially at the regions where cavitation was expected (see figure 3). The mesh consisted of 10.75 million elements with 4.4 million nodes.

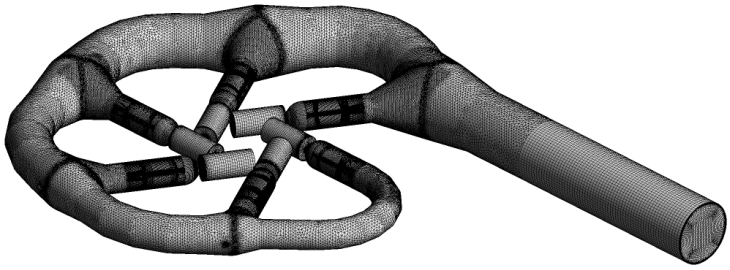

Figure 1. Computational domain and mesh for flow analysis in the manifold with injectors and jets.

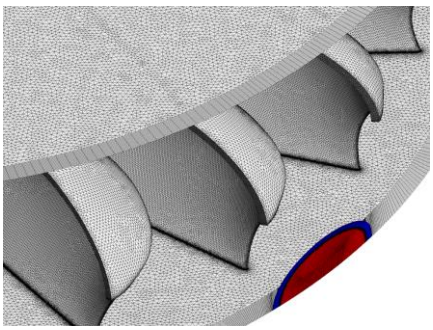

Figure 2. Detail of computational mesh for analysis of flow in the runner.

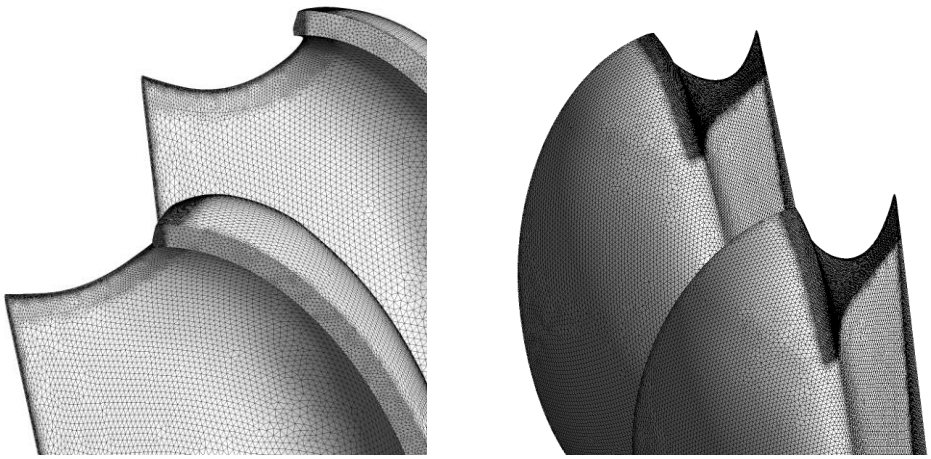

Figure 3. Details of computational mesh for cavitation prediction.
Refinement at the inner side of the bucket (left) and at the back side of the bucket (right).

3. Numerical flow simulation in a 6-jet Pelton turbine with efficiency prediction

The analysis was divided into two parts. At first, the analysis of the flow in the distributor with jets was performed. Secondly, the interaction between jets and buckets in the runner was investigated. Simulations were done for the model and for the prototype.

3.1 Flow in the distributor with injectors and jets

Proper design of the distributor with injectors is extremely important for good performance of Pelton turbines. Discharge should be equally distributed between all injectors and flow energy losses should not exceed 2% of the head. Even more important is the quality of the jets. Secondary velocities caused by bends in the distributor are highly undesirable because they can cause jet dispersion and deviation [11].

In this study a steady state analysis of the flow in the distributor with six injectors was performed with the following boundary conditions: flow rate at the inlet of the distributor, outflow with averaged static pressure at the end surfaces of the cylinders behind the nozzles (see figure 1) and opening with static pressure and air as a fluid (Air Volume Fraction = 1) on cylindrical surfaces.

The simulations were performed for the model and prototype size. Analysis of the flow in distributor was done for three needle strokes. For the model, contrary to the prototype, servomotors were outside the distributor. To check the effect of this difference between the model and the prototype, flow in distributor was analysed for both options. For maximal opening additional steady state and transient simulations were performed on refined grid. Distributor was analysed also for 1-nozzle operation. Besides flow energy losses in the distributor the quality of the jets was analysed. With this objective, the shape of the jets was checked and secondary velocities in the jets were calculated. Analysis of flow in distributor for prototype size was done mostly to get inlet conditions for runner flow simulation and it was performed only for maximal opening.

Numerical results showed that flow rate is equally distributed between the injectors. For the smallest opening the deviation from equal distribution was less than 0.1%, while for the optimal and maximal opening the deviation was less than 0.02%.

Relative flow energy losses are presented in table 1. It can be seen that in case of servomotors outside the manifold the losses are slightly higher than when the servomotors are inside the manifold. The losses are larger for small openings. The effect of mesh refinement on losses was very small and in addition with transient simulations the same values of losses were obtained. Losses for the prototype size are relatively smaller than for the model.

The quality of the jets was checked by observation of the jet shape (see figure 4) and by calculation of secondary velocities at the jet cross-section. In order to calculate secondary velocity for each injector local coordinate systems were defined in such a way that the *z* axis corresponds to the needle axis. Secondary velocity v_{sec} was then defined with the expression: $v_{sec} = \sqrt{v_x^2 + v_y^2}$.

The effect of grid refinement on the shape of the jet cross section and on the secondary velocity can be seen in figure 4. On the basic mesh the cross section of the jet is nearly a perfect circle and secondary velocity is small. With grid refinement small perturbation of the jet due to the bend of the manifold can be observed and secondary velocity increases. With transient simulation performed on the refined grid no significant difference in comparison to the steady state results on the same grid was obtained. The results are presented for the jet behind the nozzle 4, where secondary velocity is the largest. The nozzles are numbered in the direction of the flow.

Table 1. Flow energy losses in manifold, 6-nozzle operation

Configuration	**Size**	$A_0/A_{0,BEP}$	**Grid density**	**Simulation type**	**Losses** $\Delta H/H$ ***100 (%)**
Servomotor outside manifold	model	0.47	basic	steady state	1.94
Servomotor outside manifold	model	1	basic	steady state	1.27
Servomotor outside manifold	model	1.83	basic	steady state	1.23
Servomotor outside manifold	model	1.83	refined	steady state	1.20
Servomotor outside manifold	model	1.83	refined	transient, SST	1.20
Servomotor outside manifold	model	1.83	refined	transient, SAS SST	1.21
Servomotor inside nozzle	model	0.47	basic	steady state	1.89
Servomotor inside nozzle	model	1	basic	steady state	1.25
Servomotor inside nozzle	model	1.83	basic	steady state	1.16
Servomotor inside nozzle	model	1.83	refined	steady state	1.17
Servomotor inside nozzle	prototype	1.83	refined	steady state	0.84

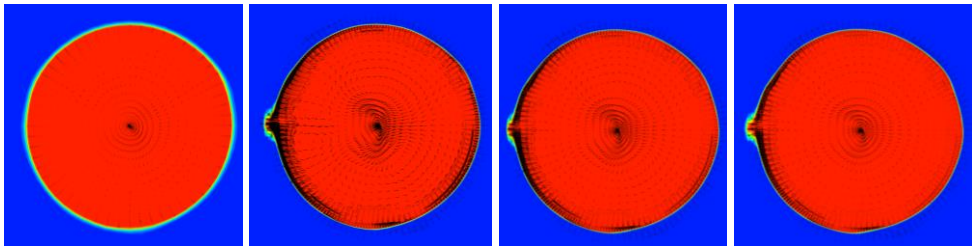

Figure 4. Shape of the jet presented with Contours of Water Volume Fraction and vectors of secondary velocities on cross-section of a jet behind the nozzle 4 (red – water, blue –air), 6-nozzle operation.
a) basic grid, steady state SST, b) refined grid, steady state SST, c) refined grid, transient SST, d) refined grid, transient SAS SST.

In table 2 results for 1-nozzle operation for maximal opening ($A_0/A_{0,BEP}$ = 1.83) are presented. As expected, flow energy losses in the manifold are the largest when the nozzle 6 is active. At the same time, for the nozzle 6 being active, the measured efficiency is the highest. This can be explained with the effect of secondary velocity in the jets on turbine performance. For nozzles 1, 2, 3, 4 and 6 negative correlation between secondary velocity and measured turbine efficiency can be clearly seen. An exception is nozzle 5, where measured efficiency was the smallest in spite of relatively small secondary velocity. 1-nozzle operation was numerically analysed also for the best efficiency point and the same negative correlation between secondary velocity and efficiency was observed, exception was

again the nozzle 5. Therefore it can be suspected that on the test rig the nozzle 5 was not accurately positioned. Nevertheless, from the results in table 2 it can be concluded, that for high turbine efficiency the quality of the jets is even more important than flow energy losses in manifold.

The results (velocity and thickness of the jets) of steady state simulations on refined mesh for model and prototype size were used as inlet boundary conditions for transient simulations in the runner.

Table 2. Results for 1-nozzle operation, $A_0/A_{0,BEP}$ =1.83
Relative flow energy losses in manifold, averaged relative secondary velocity and difference in measured efficiency for different nozzle being active. Nozzles are numbered in the flow direction.

Active nozzle	$\Delta H/H$ *100 (%)	v_{sec}/v *100 (%)	$\Delta\eta=\eta_i-\eta_6$ (%)
1	0.81	0.097	-0.06
2	0.84	0.077	-0.01
3	0.90	0.153	-0.24
4	0.92	0.195	-0.27
5	0.91	0.100	-0.38
6	0.99	0.074	0.00

3.2 Interaction between jets, buckets and evacuating water sheets in the runner and prediction of turbine efficiency

A computational domain for runner analysis consisted of two parts: a rotating part that comprises the runner and a stationary thin ring with six inlets (see figure 5a) where distribution of water and air and velocity components are prescribed. The other boundary conditions are presented in figure 5b. Time step corresponded to 0.25 degrees of runner rotation.

The results of the simulation are velocity and pressure distribution in the whole domain, as well as the shape of the jets and evacuating water sheets and an interaction between them (see figure 6).

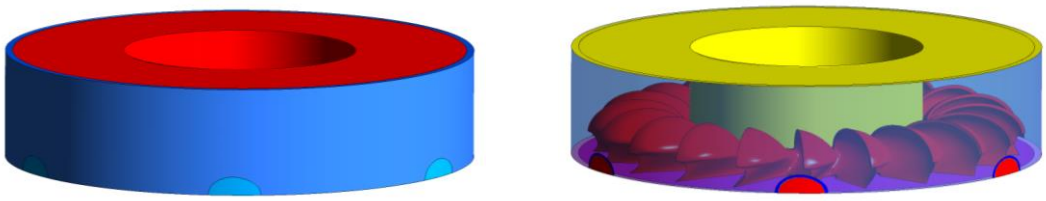

a) b)

Figure 5. Computational domain and boundary conditions.
a) rotating part (red) and stationary part with six inlet regions (blue);
b) boundary conditions: walls - red, opening - yellow, symmetry - magenta, outlet - transparent blue, inlets are coloured with Water Volume Fraction.

From pressure distribution on runner buckets torque on the shaft was calculated. At the beginning of the simulation the whole domain is filled with air and torque on the shaft is zero. During the simulation the jets get closer to the runner and when they impact the buckets the torque starts to rise. After approximately 200 time steps the value of the torque stabilizes (see figure 7), only periodic oscillation remains. For calculation of efficiency the averaged value of torque during the last 144 time steps was used.

Numerical results for the model were compared to the experimental values obtained on the test rig (see figure 8). Flow rate was input data, therefore its numerical and experimental values are the same. Numerical values of head, torque and efficiency are smaller than the experimental ones. The largest

discrepancy is for the value of torque, where calculated value is 3.51% smaller than the measured one. Efficiency was calculated also for the prototype size, the value was 0.11% higher than for the model.

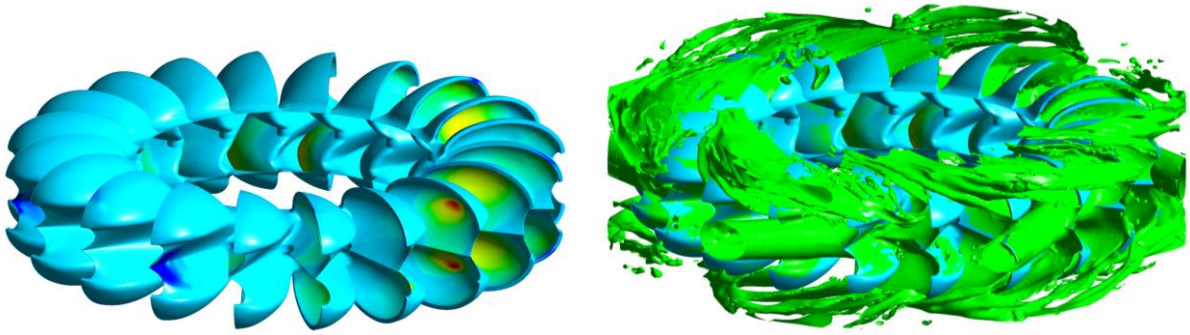

Figure 6. Pressure distribution on the buckets (left) and water jets and evacuating water sheets presented as isosurface of Water Volume Fraction = 0.5 (right).

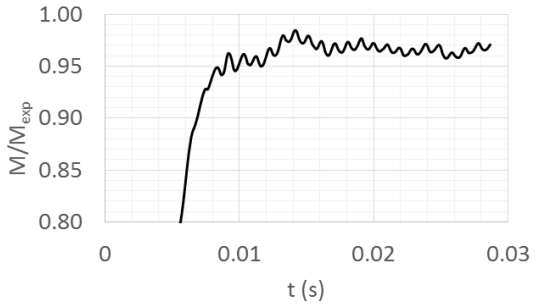

Figure 7. Torque on the shaft during the simulation, model size, 6-nozzle operation, $A_0/A_{0,BEP}$ = 1.83.

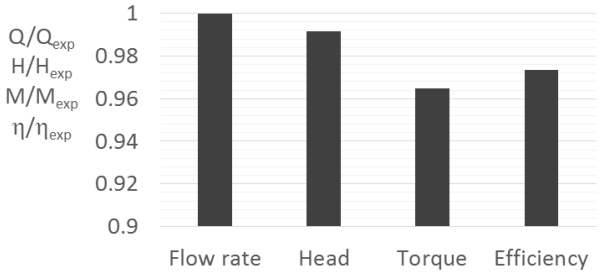

Figure 8. Comparison of numerical results to the experimental values, model size, 6-nozzle operation, $A_0/A_{0,BEP}$ = 1.83.

For the prototype two simulations of flow in the runner were performed: one with only one nozzle active and the other for 6-nozzle operation, both for $A_0/A_{0,BEP}$ = 1.83.

For the prototype a detailed analysis of results during several time steps was done. In figure 9 it can be seen that evacuating water sheets do not impact the previous buckets. Special attention was paid to check possible interaction between the evacuating water sheets and the jets. The results at several time steps were carefully analysed. In figure 10 iso-surfaces with 30% of water (Water Volume Fraction = 0.3) are presented for two time steps. On the left part of the pictures the iso-surfaces are coloured by water velocity, while on the right part they are coloured by wall distance. Discontinuity in colour shows that there is a gap between the jet and the evacuating water. So there is no interaction between the evacuating water sheets and the approaching jet, although the bucket is never empty.

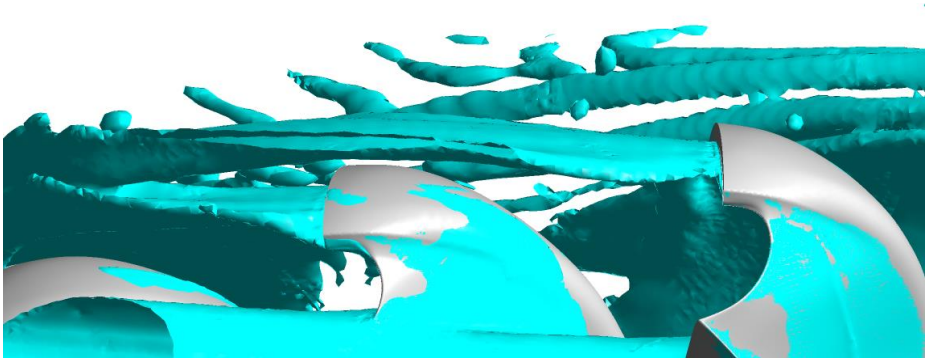

Figure 9. Iso-surface of Water Volume Fraction = 0.3. Prototype size, 6-nozzle operation.

In figure 11 contribution of one bucket to the complete torque on the shaft is presented for 1-nozzle and 6-nozzle operation. For 1-nozzle operation the bucket contributes to the torque during approximately 90 degrees of runner revolution. For 6-nozzle operation before all the water leaves the bucket the next jet impacts it. Therefore during 6-nozzle operation at each moment all the buckets contribute to the torque (see figure 12). The runner consists of 20 buckets and there are 6 jets, therefore $M_i = M_{i+10}$, where M_i is the contribution of bucket #i to the torque.

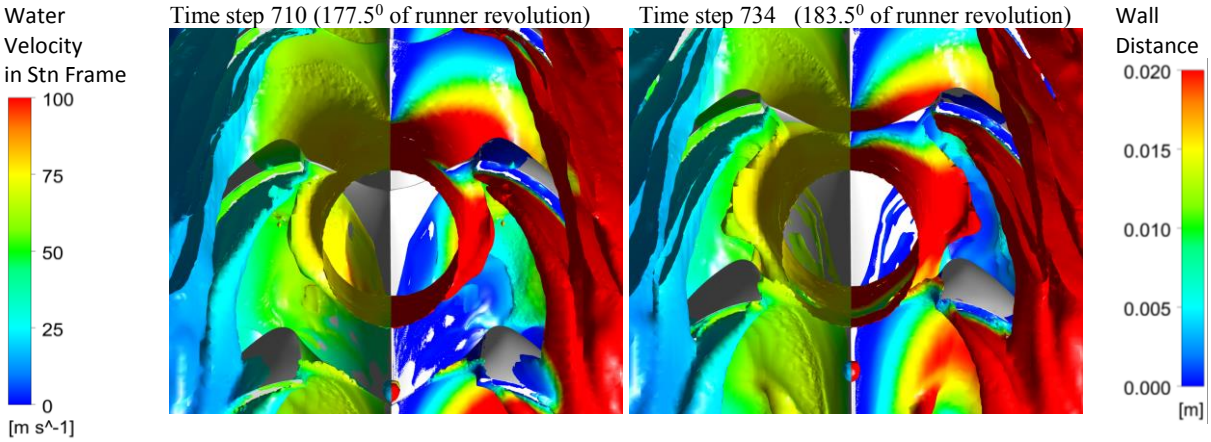

Figure 10. Water jets and evacuating water sheets presented by iso-surface of Water Volume Fraction = 0.3. Left half is coloured by water velocity, while the right half of the pictures is coloured by wall distance.

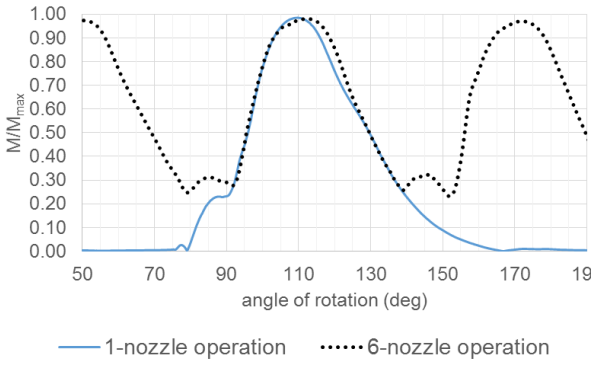

Figure 11. Contribution of one bucket to the torque on the shaft, prototype size, 1-nozzle and 6-nozzle operation.

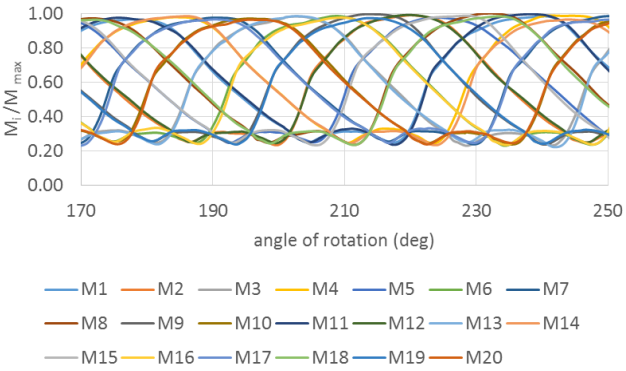

Figure 12. Contributions of all buckets to the torque on the shaft, prototype size, 6-nozzle operation.

4 Cavitation prediction

Cavitation prediction was done for a prototype of a 2-jet high head Pelton turbine with runner diameter D = 1.2 m. The runner consists of 20 buckets.

Prediction of cavitation in a Pelton turbine is very time consuming. Three-component flow consisting of water, water vapour and air has to be modelled. For close observation of formation and decay of water vapour cavities, a very small time step is needed. Furthermore, double precision of calculation has to be used, in order to improve the accuracy of the results and to avoid sudden overflows due to accumulation of numerical errors. Since the simulation of the entire runner is too time consuming, in this case the simulation was reduced to five runner buckets (see figure 13). Due to

the symmetry the computational domain was reduced to one half. At the inlet the velocity and thickness of the jet obtained in previous numerical analysis of the flow in distributor with injectors and jets (as in section 3.1) were prescribed.

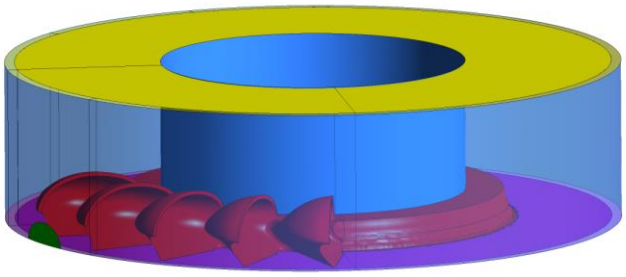

Figure 13. Computational domain for cavitation prediction. The position of the buckets at the beginning of the simulation.
magenta – symmetry condition, red – runner, yellow – wall, green – inlet, blue – opening.

At the beginning of the simulation the whole computational domain was filled with air. It took some time before the jet impacted the first bucket, therefore the first 36 degrees of runner rotation were performed without cavitation modelling. For this part of the simulation the time step was equal to the time needed for 0.5 deg. of runner revolution. After the 36 deg. of runner revolution the cavitation was included. Time step was reduced to 0.1 deg. of runner revolution and additional 360 time steps were performed.

The presence of water vapour does not necessarily cause material erosion. For cavitation pitting water vapour cavity has to be in contact with the bucket surface and the condensation has to be very fast without presence of air. For numerical simulations Rossetti at al. in [9] suggested three practical conditions for cavitation pitting:

- at time t* a cavity with at least 80% of water vapour is stuck to the bucket,
- at time t*+Δt less than 20% of water vapour is in the cavity, where $\Delta t \leq 40\mu s$,
- during the condensation process less than 10% of air is in the mixture of fluids in contact with the vapour cavity.

To check these conditions for cavitation pitting we closely observed the formation and the decay of water vapour cavities at different time steps. In figures 14 and 15 cavitation at the inner and the back side of the buckets is presented. Water vapour is coloured with wall distance in order to see if vapour is stuck to the bucket and how thick the vapour cavity is. Water jets and evacuating water sheets are presented with transparent red, so it can be seen if vapour is inside the jet or if it is in contact with air.

At the inner side of the bucket a small cavity with less than 40% of water vapour was observed (see figure 14). The condensation was very slow, more than 0.0018 seconds was needed before the vapour entirely disappeared. Therefore the conditions for cavitation pitting are not fulfilled.

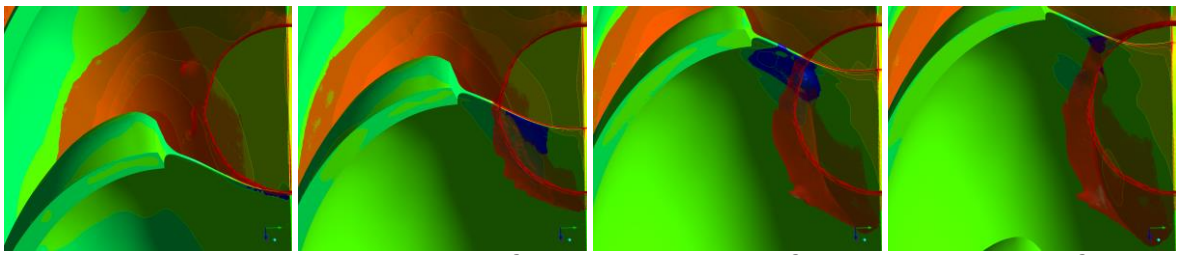

t* t* + 0.74 .10^{-3}s t* + 1.48 .10^{-3}s t* + 1.85 .10^{-3}s

Figure 14. Cavitation at the inner side of the bucket.
Water is presented with iso-surface of Water Volume Fraction = 0.5 in transparent red.
Water vapour is presented with iso-surfaces of Vapour Volume Fraction = 0.2 coloured with Wall Distance (dark blue).

The second cavity of water vapour was observed at the backside of the bucket. Its development and condensation is presented in figure 15. In the first three pictures the region with water vapour enlarges. At the fourth picture the condensation started at the nib of the knife. The condensation is faster than at the inner side of the bucket but the water vapour is in contact with air, therefore no erosion of material is expected.

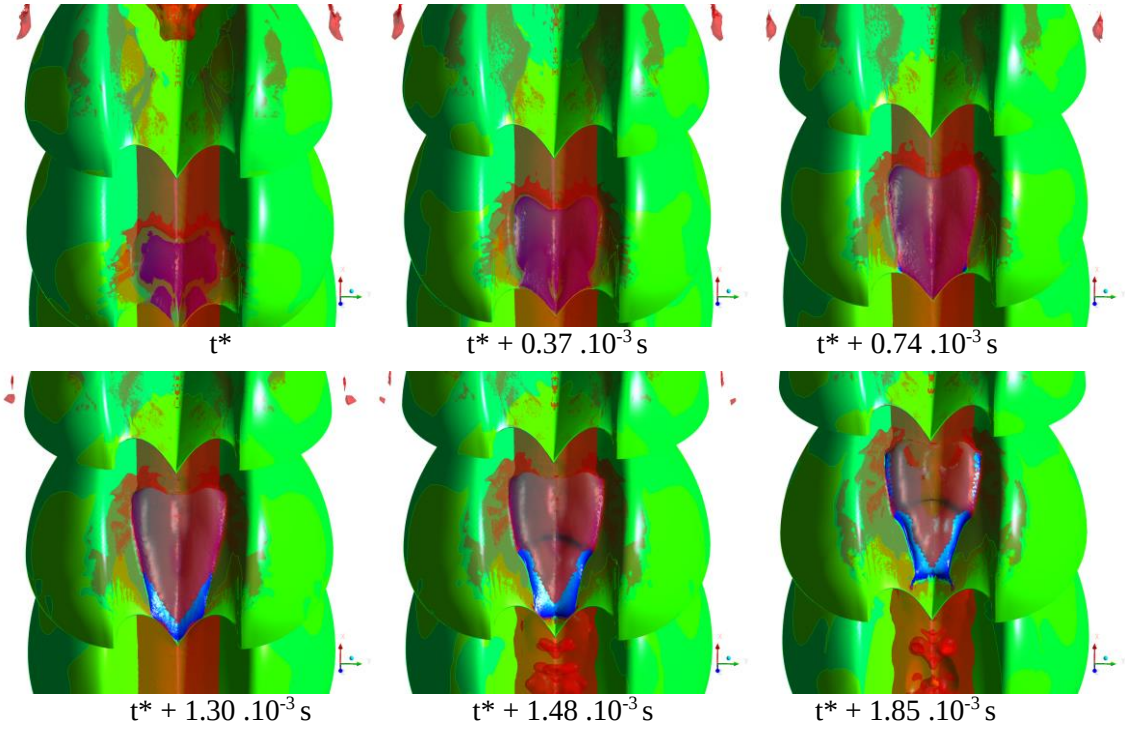

Figure 15. Cavitation at the back side of the bucket.
Water is presented with iso-surface of Water Volume Fraction = 0.8 in transparent red.
Water vapour is presented with iso-surfaces of Vapour Volume Fraction = 0.5 coloured with Wall Distance.

5 Conclusions

Numerical simulation can be a useful tool for qualitative and quantitative analysis of Pelton turbines. On the basis of numerical results efficiency and cavitation can be predicted. In the first part of this paper the following results for the 6-jet Pelton turbine are presented:

- Flow energy losses in the distributor were calculated. The effect of grid density on predicted quality of the jets was presented. From the results for 1-nozzle operation a negative correlation between secondary velocity in the jets and turbine efficiency was obtained.
- Numerically predicted torque on the shaft and turbine efficiency were in good agreement with the results from the test rig.
- Qualitative analysis of the results for the prototype size proved that there is no interaction between evacuating water sheets and the jets. As well, water evacuating from the buckets does not get in contact with the previous buckets.

In the second part the cavitation prediction for a prototype of a high head 2-jet Pelton turbine was presented. Two regions with water vapour were observed. The first one was at the inner side of the buckets near the cut-out, but the concentration of vapour was small and the condensation process was very slow. The second region with water vapour was at the back side of the bucket. Also there the

condensation process was rather slow and water vapour was in contact with air. So it can be concluded that the conditions for cavitation pitting are not fulfilled and no cavitation damages are expected.

Acknowledgements
The research leading to these results has received funding from the People Programme (Marie Curie Actions) of the European Union's Seventh Framework Programme FP7/2007-2013/ under REA grant agreement n°612279 and from the Slovenian Research Agency ARRS - Contracts No. 1000-15-0263 and P2-0196.

Nomenclature

A_0	Relative opening [-]
$A_{0,\,BEP}$	Relative opening at BEP [-]
H	Head [m]
M	Torque on the shaft
Mi	Contribution of bucket #i to the torque on the shaft
Q	Flow rate [m^3/s]
Q_i	Flow rate through nozzle #i [m^3/s]
v	Velocity [m/s]
v_{sec}	Secondary velocity in the jet [m/s]
ΔH	Flow energy losses [m]
η	Turbine efficiency
η_i	Turbine efficiency, active only nozzle i
η_{BEP}	Turbine efficiency at BEP
η_{rel}	Relative efficiency [-], ($=\eta / \eta_{BEP}$)

Subscripts:

exp	experimental values

Abbreviations:

BEP	Best Efficiency Point
CFD	Computational Fluid Dynamic
SST	Shear Stress Transport
SAS	Scale Adaptive Simulation

References

[1] Parkinson E, Garcin H, Vullioud G, Zhang Z, Muggli F and Casartelli E 2002 Experimental and numerical investigation of the free jet flow at a model nozzle of a Pelton turbine *Proceedings of the XX1st IAHR Symposium on Hydraulic Machinery and Systems (Lausanne)*
[2] Kvicinsky S, Kueny J-L, Avellan F and Parkinson E 2002 Experimental and numerical analysis of free surface flows in a rotating bucket *Proceedings of the XX1st IAHR Symposium on Hydraulic Machinery and Systems (Lausanne)*
[3] Mack R and Moser W 2002 Numerical investigation of the flow in a Pelton turbine *Proceedings of the XXIst IAHR Symposium on Hydraulic Machinery and Systems (Lausanne)*
[4] Perrig A 2007 Hydrodynamics of the free surface flow in Pelton turbine buckets *Ph. D. Thesis No. 3715*, (Lausanne: École polytechnique fédérale de Lausanne)
[5] Jošt D, Mežnar P and Lipej A 2010 Numerical prediction of Pelton turbine efficiency *IOP Conf. Ser.: Earth Environ. Sci.* **12** 012080
[6] Santolin A, Cavazzini G, Ardizzon G and Pavesi G 2009 Numerical investigation of the interaction between jet and bucket in a Pelton turbine *Proc. Inst. of Mech. Engineers Part A, J. Power Energy* **223(6)** pp 721–8
[7] Marongiu J, Leboeuf F, Caro J and Parkinson E 2010 Free surface flows simulations in Pelton turbines using an hybrid SPH-ALE Method *J. Hydraulic Res.* **48** sup1 pp 40-9
[8] Vessaz C, Jahanbaksh E and Avellan F 2015 Flow simulation of jet deviation by rotating Pelton buckets using finite volume particle method *J. Fluids Eng.* **137(7)** 074501
[9] Rosetti A, Pavesi G, Ardizzon G and Santolin A 2014 Numerical analyses of cavitating flow in a Pelton turbine *J. Fluids Eng.* **136(8)** 081304
[10] Zwart P J, Gerber A G and Belamri T 2004 A two-phase model for predicting cavitation dynamics *Fifth International Conference on Multiphase Flow* (Yokohama)
[11] Staubli T, Abgottspon A, Weibel P, Bissel C, Parkinson E, Leduc J and Leboeuf F 2009 Jet quality and Pelton efficiency *Hydro 2009* (Lyon)